Wiadomości Lekarskie
Medical Advances

VOLUME LXXVI, ISSUE 10, OCTOBER 2023
Official journal of Polish Medical Association has been published since 1928

ISSN 0043-5147
E-ISSN 2719-342X

INDEXED IN PUBMED/MEDLINE, SCOPUS, EMBASE, EBSCO, INDEX COPERNICUS,
POLISH MINISTRY OF EDUCATION AND SCIENCE, POLISH MEDICAL BIBLIOGRAPHY

ORIGINAL ARTICLE

MICROCIRCULATORY ALTERATIONS IN STABLE CORONARY ARTERY DISEASE PATIENTS WITH CONCOMITANT COVID-19

DOI: 10.36740/WLek202310115

Vasyl Z. Netiazhenko[1, 2], Serhii I. Mostovyi[1, 3], Olga M. Safonova[4], Kyrylo O. Mikhaliev[2]

[1] BOGOMOLETS NATIONAL MEDICAL UNIVERSITY, KYIV, UKRAINE

[2] STATE INSTITUTION OF SCIENCE «RESEARCH AND PRACTICAL CENTER OF PREVENTIVE AND CLINICAL MEDICINE» STATE ADMINISTRATIVE DEPARTMENT, KYIV, UKRAINE

[3] SE «MEDBUD», KYIV, UKRAINE

[4] KYIV CITY CLINICAL HOSPITAL NO. 18, KYIV, UKRAINE

ABSTRACT

The aim: To evaluate the alterations in microcirculation of stable coronary artery disease (SCAD) patients with concomitant COVID-19.

Materials and methods: The cross-sectional study analyzed the data from 80 patients, being subdivided as follows: group 1 (G_1) – SCAD without COVID-19 (n=30); group 2 (G_2) – SCAD with concomitant COVID-19 (n=25); group 3 (G_3) – COVID-19 without SCAD (n=25). The control group included 30 relatively healthy volunteers. The state of microcirculation was assessed by nailfold videocapillaroscopy (NVC) and laser Doppler flowmetry (LDF).

Results: NVC data from G_2 revealed the sings of capillary bed remodeling, along with the most pronounced decrease in capillary (arteriolar part of the loop) blood flow velocity (vs. G_1 and G_3). LDF data from G_2 were evident for the alterations in both endothelium-dependent and -independent mechanisms of microvascular flow regulation. The 72 % of G_2 constituted the cases of microcirculatory hemodynamic «congestion-stasis» (MHCS) type (characterized by the decreased laser Doppler perfusion index and reduced endothelium-dependent microvascular reactivity [MVR]), and the cases of mixed type with reduced MVR. The pooled hyporeactive profile (of both MHCS type and a mixed type with reduced MVR) demonstrated the higher frequency of G_2 patients (40 %), as against 11 % in the pooled alternative hemodynamic group ($p<0,001$) (included 80 % of cases with preserved MVR).

Conclusions: G_2 profile demonstrated the predomination of patients, possessing a MHCS type or a mixed type with reduced MVR. The pooled microcirculatory hyporeactive profile was presented with G_2 cases to a greater extent, than in the pooled profile with predominantly preserved MVR.

KEY WORDS: SARS-CoV-2 infection, COVID-19, myocardial ischemia, microcirculation

Wiad Lek. 2023;76(10):2224-2238

INTRODUCTION

To date, it has been clearly established, that the coronavirus disease (COVID-19), caused by severe acute respiratory syndrome coronavirus type 2 (SARS-CoV-2), mostly affecting a respiratory system, simultaneously induces a multi-organ damage, which, in its turn, is associated with an increased risk of severe complicated course of SARS-CoV-2 infection [1].

While discussing a COVID-19 as a multifaceted systemic disorder, it is worth mentioning that SARS-CoV-2 negatively impacts on the microcirculation, involving the series of underlying pathomechanisms, particularly the endothelial damage, microthrombosis and microvascular occlusion [2, 3]. Of note, the microvascular alterations are considered not only as a pathophysiological aspect within the framework of acute SARS-CoV-2 infection, but also as a factor associated with the increased risk of long-term postinfection sequelae in COVID-19 convalescents [4].

The growing body of evidence suggests that the patients with pre-existing cardiovascular comorbidities are more prone to COVID-19-related complications and subjected to higher associated mortality [5]. In particular, the coronary artery disease is linked to SARS-CoV-2 infection in a manner of mutually aggravation [5-7]. Moreover, the microvascular alterations, including the endothelial dysfunction and damage, are likely to be the factors, significantly contributing to such a dramatic reciprocal deterioration of both conditions` course [8, 9].

At present, the methodology of non-invasive study of peripheral microcirculation, specifically in COVID-19 patients or convalescents, includes the use of nailfold (video)cappilaroscopy (NVC) [10, 11]

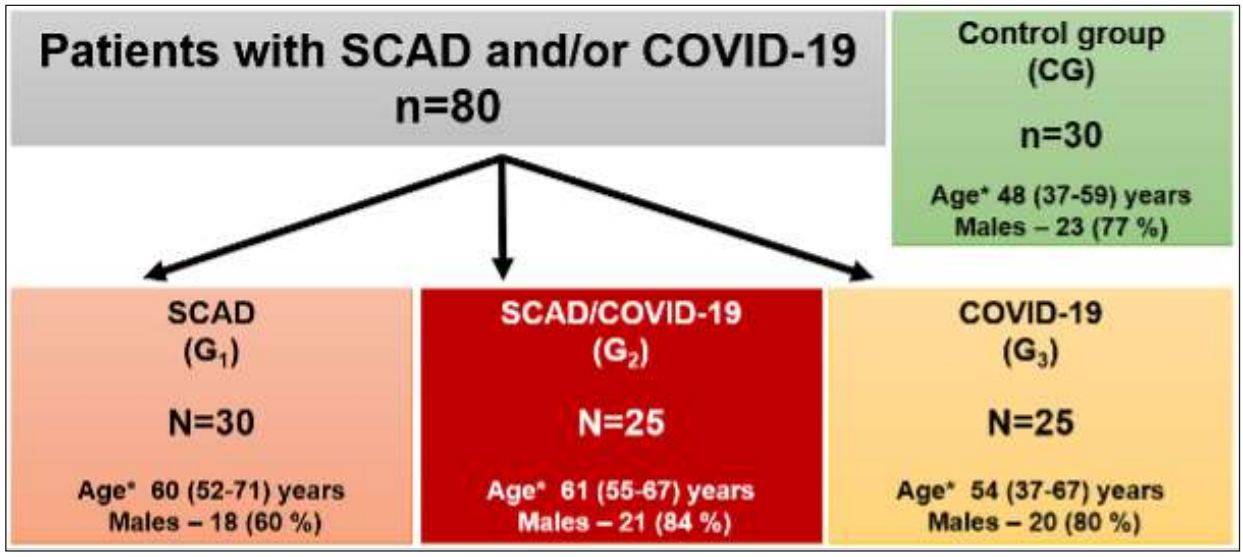

Fig. 1. The present study design. * – Median (Me), interquartile range (IQR).

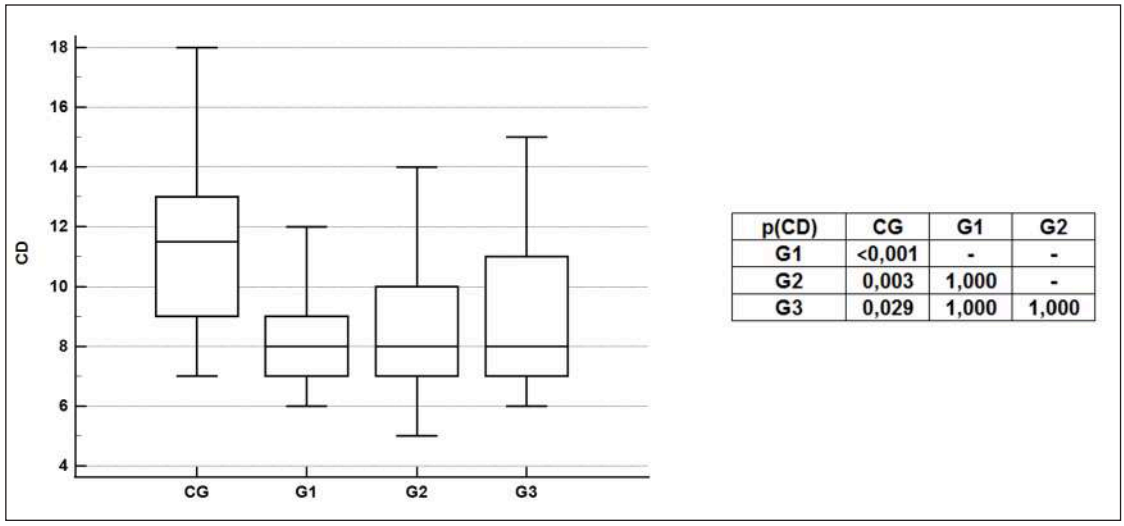

p(CD)	CG	G1	G2
G1	<0,001	-	-
G2	0,003	1,000	-
G3	0,029	1,000	1,000

Fig. 2. CD (per 1 mm^2) in G_1-G_3 patients and controls (box-and-whiskey plots; the significance of difference (p[CD]) between the studied groups)

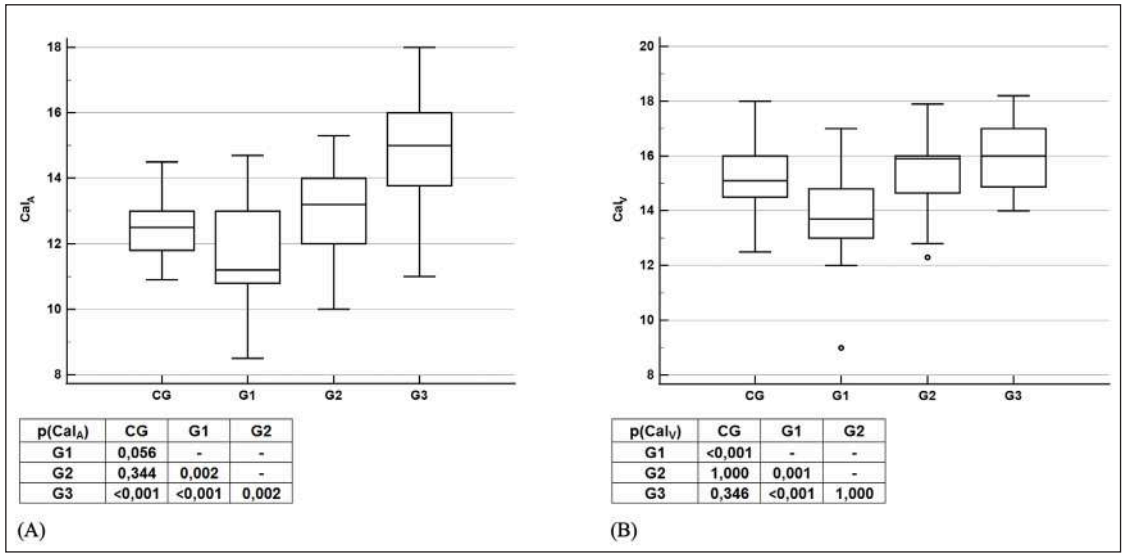

p(CalA)	CG	G1	G2
G1	0,056	-	-
G2	0,344	0,002	-
G3	<0,001	<0,001	0,002

p(CalV)	CG	G1	G2
G1	<0,001	-	-
G2	1,000	0,001	-
G3	0,346	<0,001	1,000

Fig. 3. Cal_A (A) and Cal_V (μm) (B) in G_1-G_3 patients and CG (box-and-whiskey plots; the significance of difference (p[Cal_A] and p[Cal_V], respectively) between the studied groups)

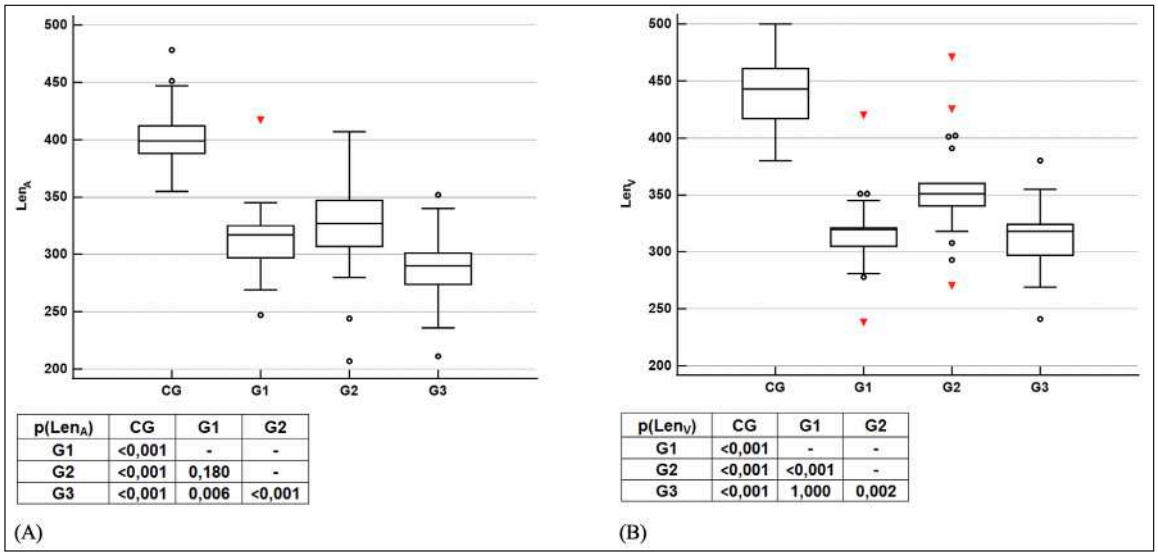

p(Len$_A$)	CG	G1	G2
G1	<0,001	-	-
G2	<0,001	0,180	-
G3	<0,001	0,006	<0,001

p(Len$_V$)	CG	G1	G2
G1	<0,001	-	-
G2	<0,001	<0,001	-
G3	<0,001	1,000	0,002

Fig. 4. Len$_A$ (A) and Len$_V$ (μm) (B) in G$_1$-G$_3$ patients and CG (box-and-whiskey plots; the significance of difference (p[Len$_A$] and p[Len$_V$], respectively) between the studied groups)

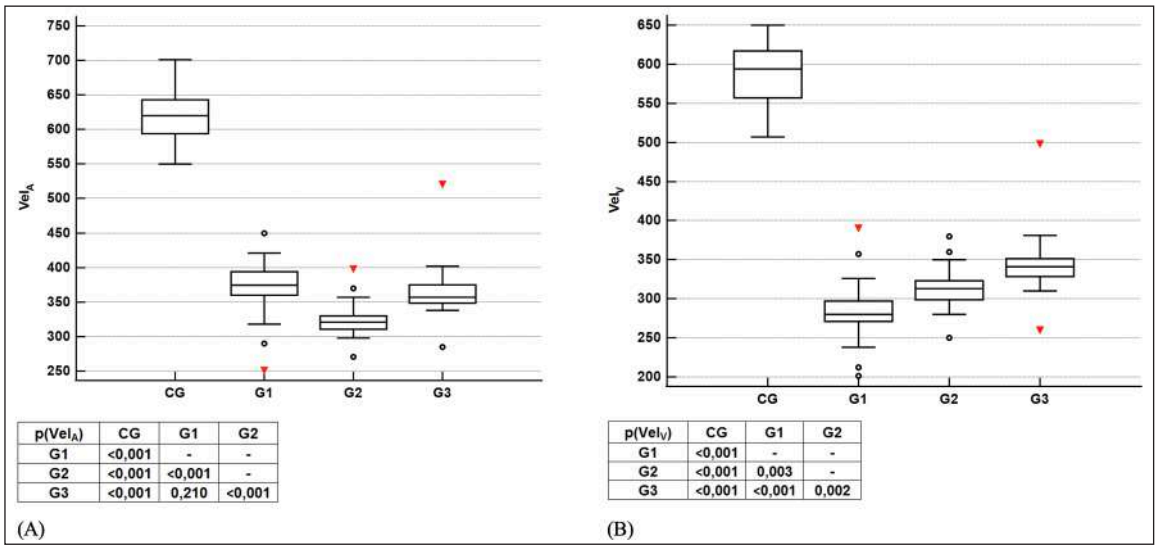

p(Vel$_A$)	CG	G1	G2
G1	<0,001	-	-
G2	<0,001	<0,001	-
G3	<0,001	0,210	<0,001

p(Vel$_V$)	CG	G1	G2
G1	<0,001	-	-
G2	<0,001	0,003	-
G3	<0,001	<0,001	0,002

Fig. 5. Vel$_A$ (A) and Vel$_V$ (μm) (B) in G$_1$-G$_3$ patients and CG (box-and-whiskey plots; the significance of difference (p[Vel$_A$] and p[Vel$_V$], respectively) between the studied groups)

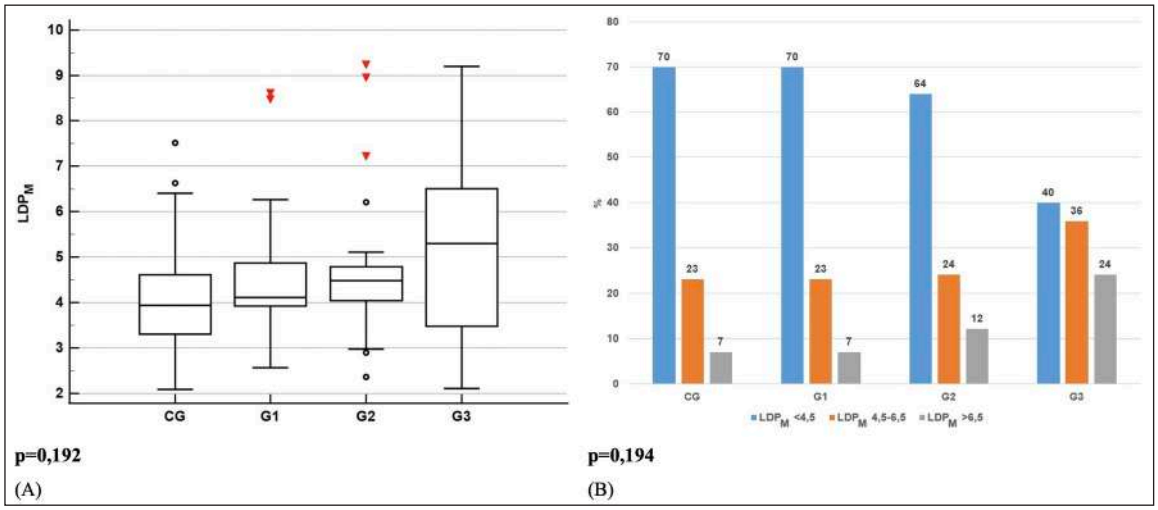

Fig. 6. Baseline LDP$_M$ (a.u.) in G$_1$-G$_3$ patients and controls (A – box-and-whiskey plots; B – the structure of LDP$_M$ patterns (a.u.) in the studied groups).

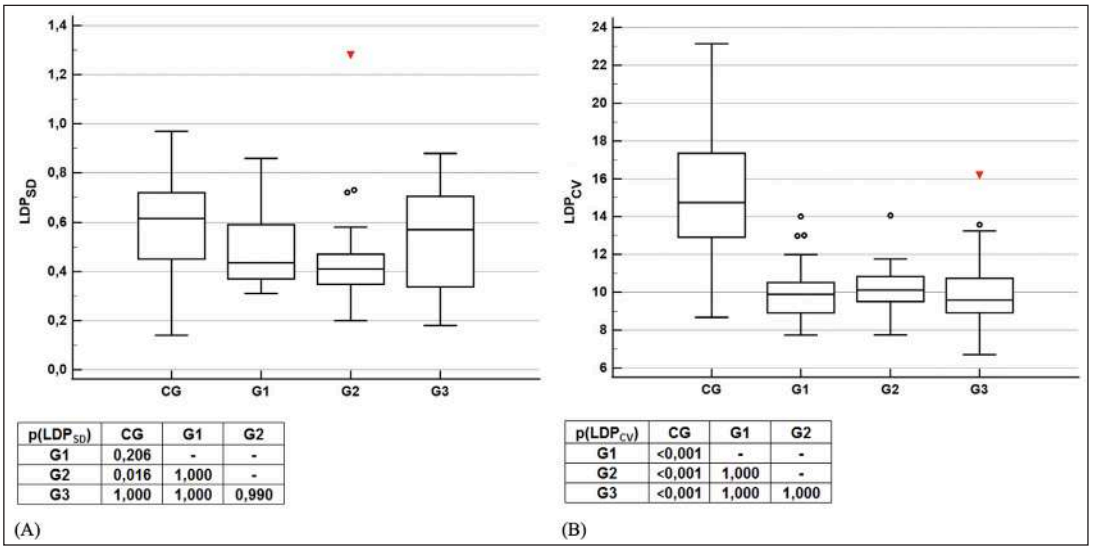

p(LDP$_{SD}$)	CG	G1	G2
G1	0,206	-	-
G2	0,016	1,000	-
G3	1,000	1,000	0,990

p(LDP$_{CV}$)	CG	G1	G2
G1	<0,001	-	-
G2	<0,001	1,000	-
G3	<0,001	1,000	1,000

Fig. 7. Baseline LDP variability in G_1-G_3 patients and controls (A – SD (a.u.); box-and-whiskey plots; the significance of difference (p[LDP_{SD}]) between the studied groups; B – CV (%); box-and-whiskey plots; the significance of difference (p[LDP_{CV}]) between the studied groups).

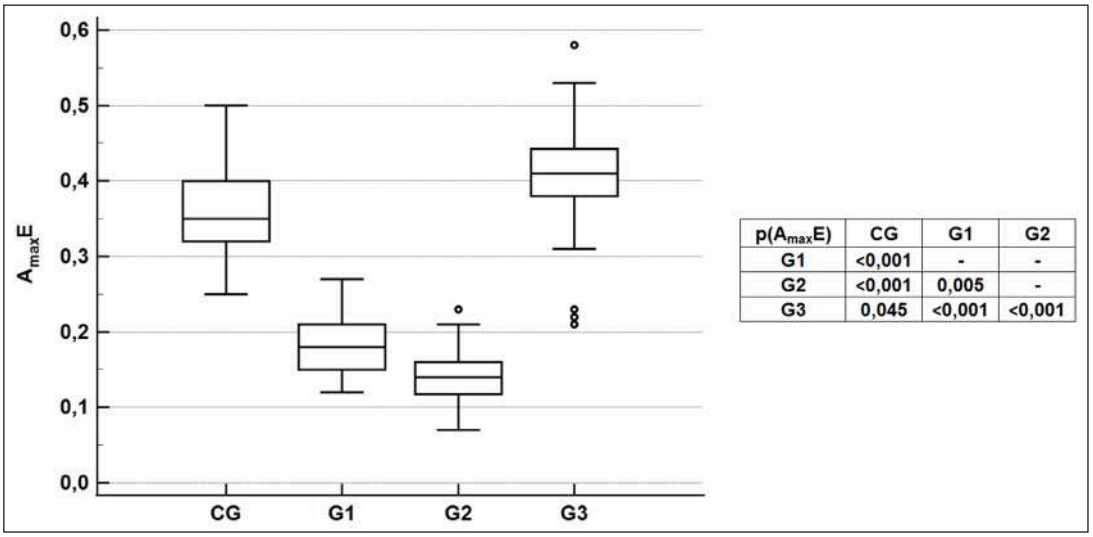

p(A_{max}E)	CG	G1	G2
G1	<0,001	-	-
G2	<0,001	0,005	-
G3	0,045	<0,001	<0,001

Fig. 8. A_{max}E (Hz) in G_1-G_3 patients and CG (box-and-whiskey plots; the significance of difference (p[A_{max}E]) between the studied groups)

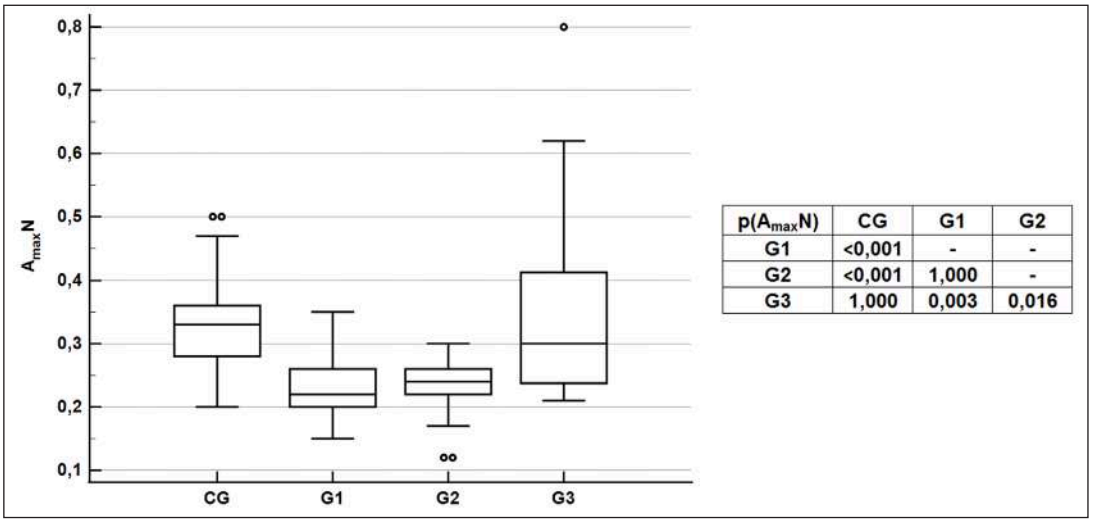

p(A_{max}N)	CG	G1	G2
G1	<0,001	-	-
G2	<0,001	1,000	-
G3	1,000	0,003	0,016

Fig. 9. A_{max}N (Hz) in G_1-G_3 patients and CG (box-and-whiskey plots; the significance of difference (p[A_{max}N]) between the studied groups)

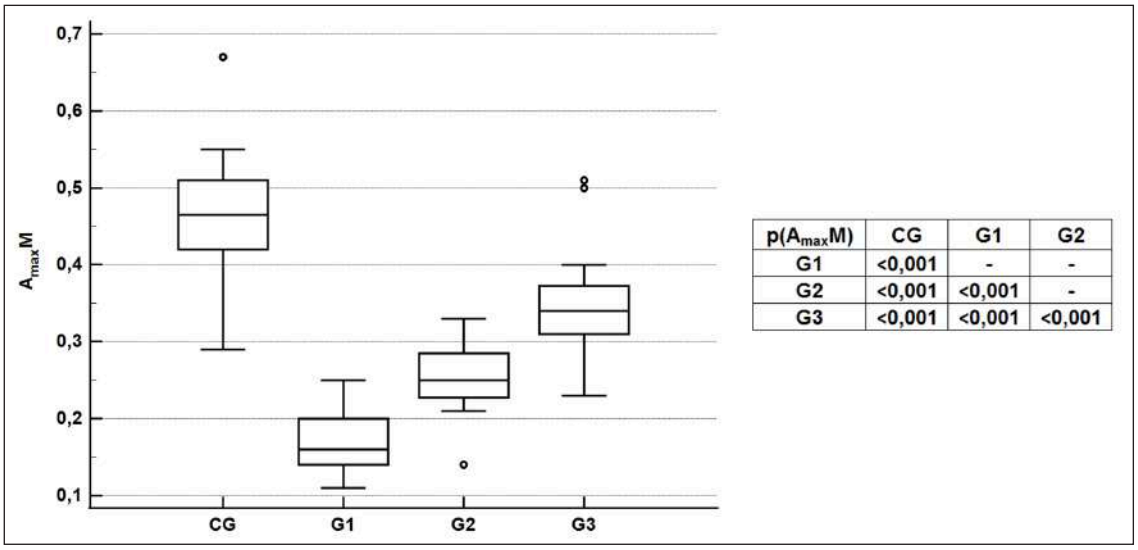

p(A_{max}M)	CG	G1	G2
G1	<0,001	-	-
G2	<0,001	<0,001	-
G3	<0,001	<0,001	<0,001

Fig. 10. A_{max}M (Hz) in G_1-G_3 patients and CG (box-and-whiskey plots; the significance of difference (p[A_{max}M]) between the studied groups)

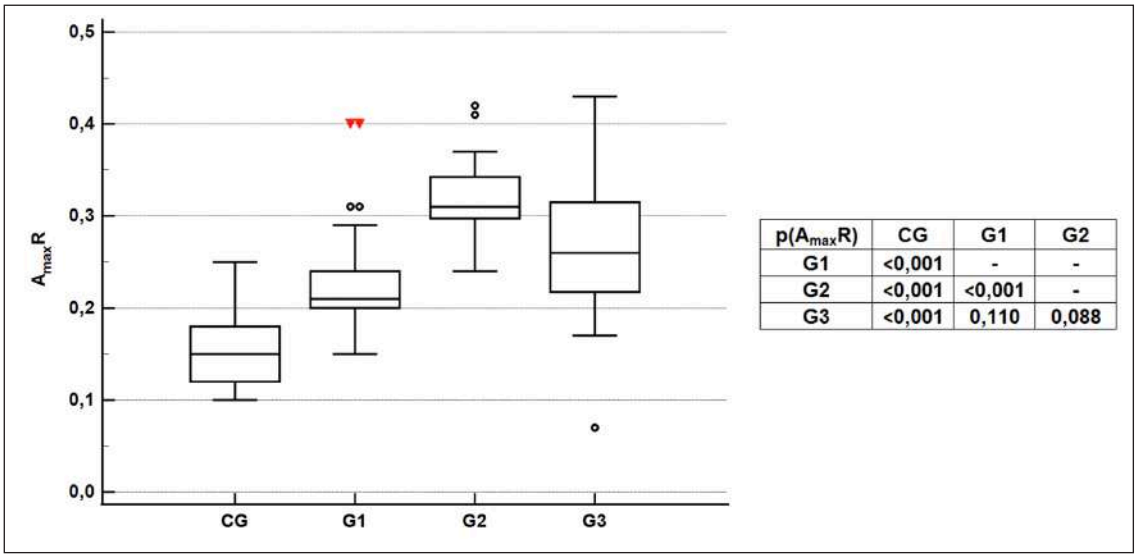

p(A_{max}R)	CG	G1	G2
G1	<0,001	-	-
G2	<0,001	<0,001	-
G3	<0,001	0,110	0,088

Fig. 11. A_{max}R (Hz) in G_1-G_3 patients and CG (box-and-whiskey plots; the significance of difference (p[A_{max}R]) between the studied groups)

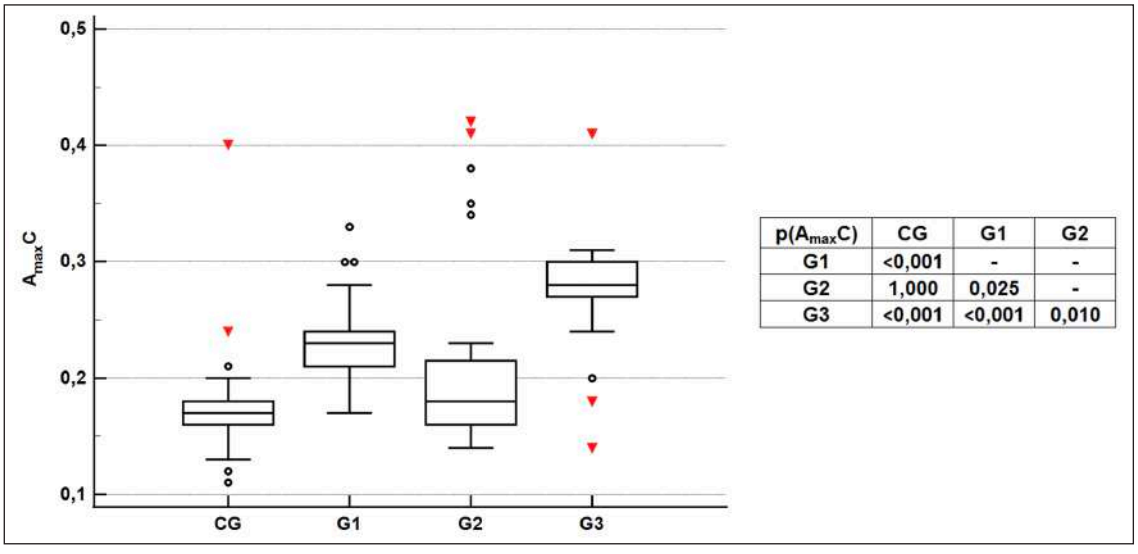

p(A_{max}C)	CG	G1	G2
G1	<0,001	-	-
G2	1,000	0,025	-
G3	<0,001	<0,001	0,010

Fig. 12. A_{max}C (Hz) in G_1-G_3 patients and CG (box-and-whiskey plots; the significance of difference (p[A_{max}C]) between the studied groups)

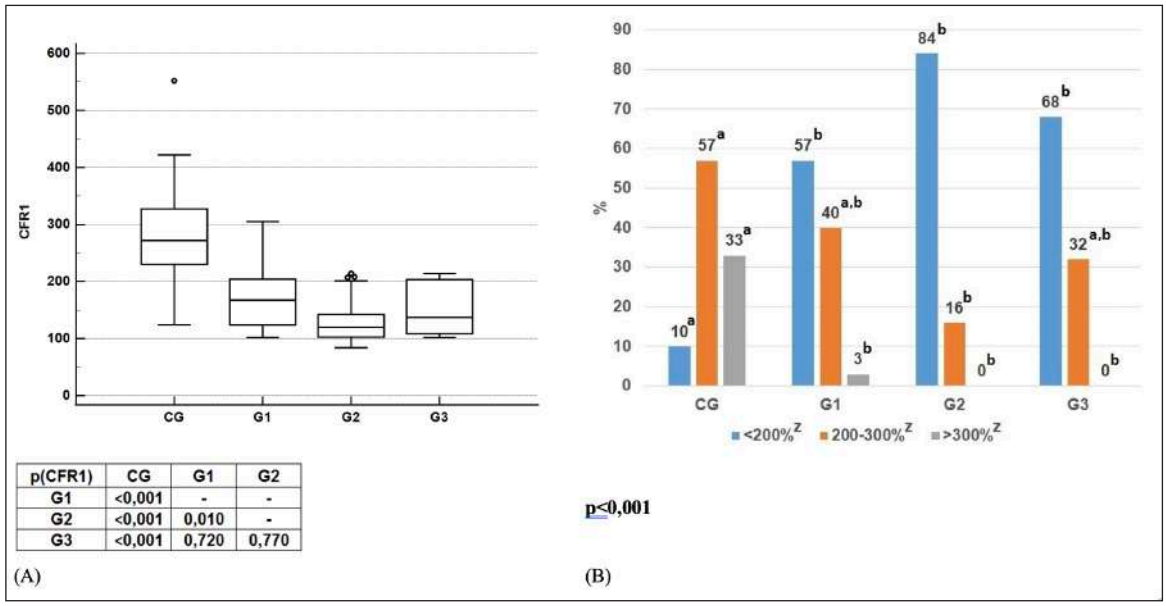

p(CFR1)	CG	G1	G2
G1	<0,001	-	-
G2	<0,001	0,010	-
G3	<0,001	0,720	0,770

Fig. 13. CFR1 (%) in G_1-G_3 patients and controls (A – box-and-whiskey plots and the significance of difference (p[CFR1]) between the studied groups; B – the structure of CFR1 patterns in the studied groups). ^{z} – Statistically significant difference by z-test. ^{a,b} – Each subscript letter denotes the subsets of the corresponding studied groups, whose column proportions do not differ significantly from each other at p<0,05.

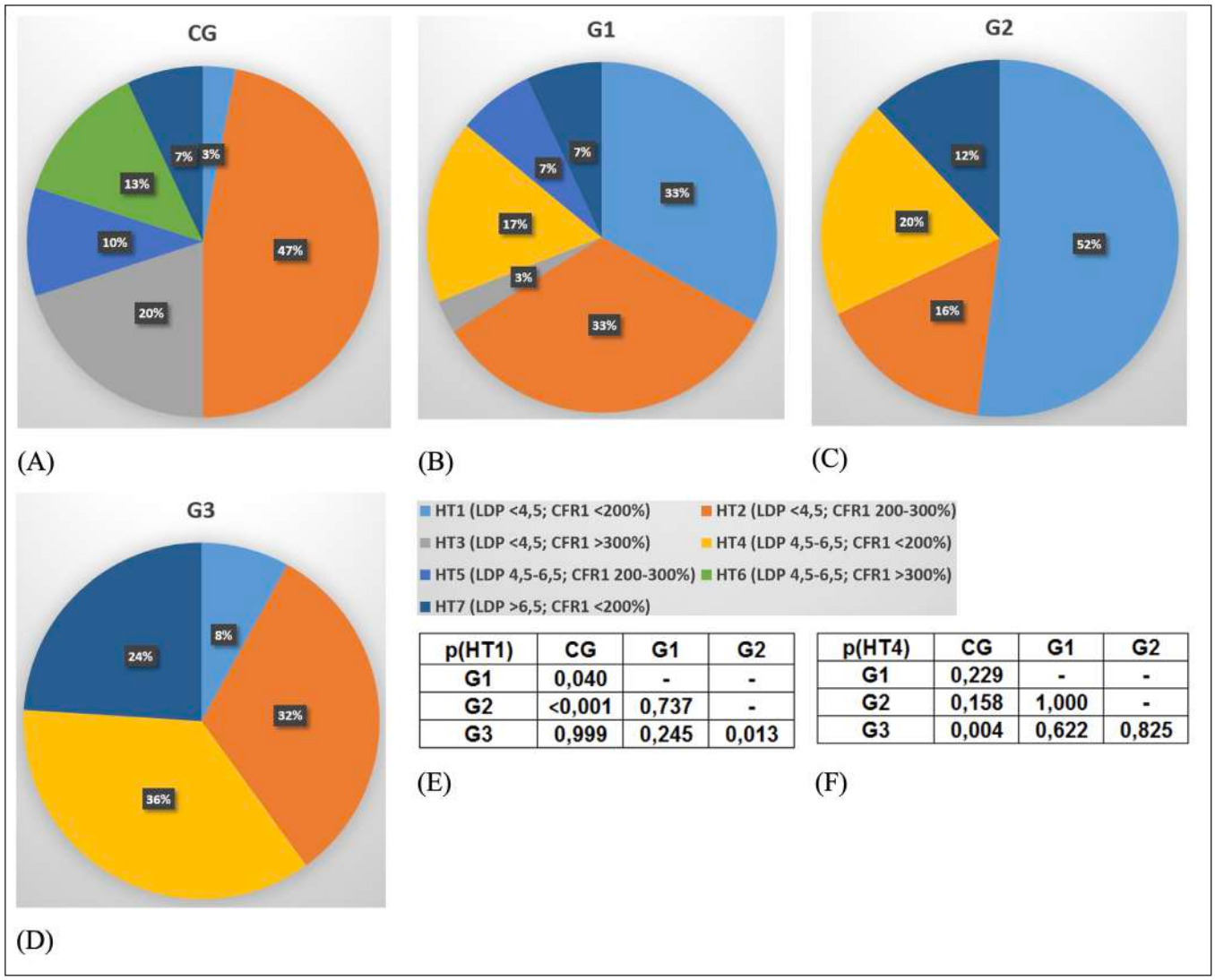

p(HT1)	CG	G1	G2
G1	0,040	-	-
G2	<0,001	0,737	-
G3	0,999	0,245	0,013

(E)

p(HT4)	CG	G1	G2
G1	0,229	-	-
G2	0,158	1,000	-
G3	0,004	0,622	0,825

(F)

Fig. 14. Hemodynamic types (HTs) of microcirculation in G_1-G_3 patients and controls (A-D: the structure of HTs (%) in CG and G_1-G_3; E – the significance of difference (p[HT1]) between the studied groups by HT1 frequency; F – the significance of difference (p[HT4]) between the studied groups by HT4 frequency)

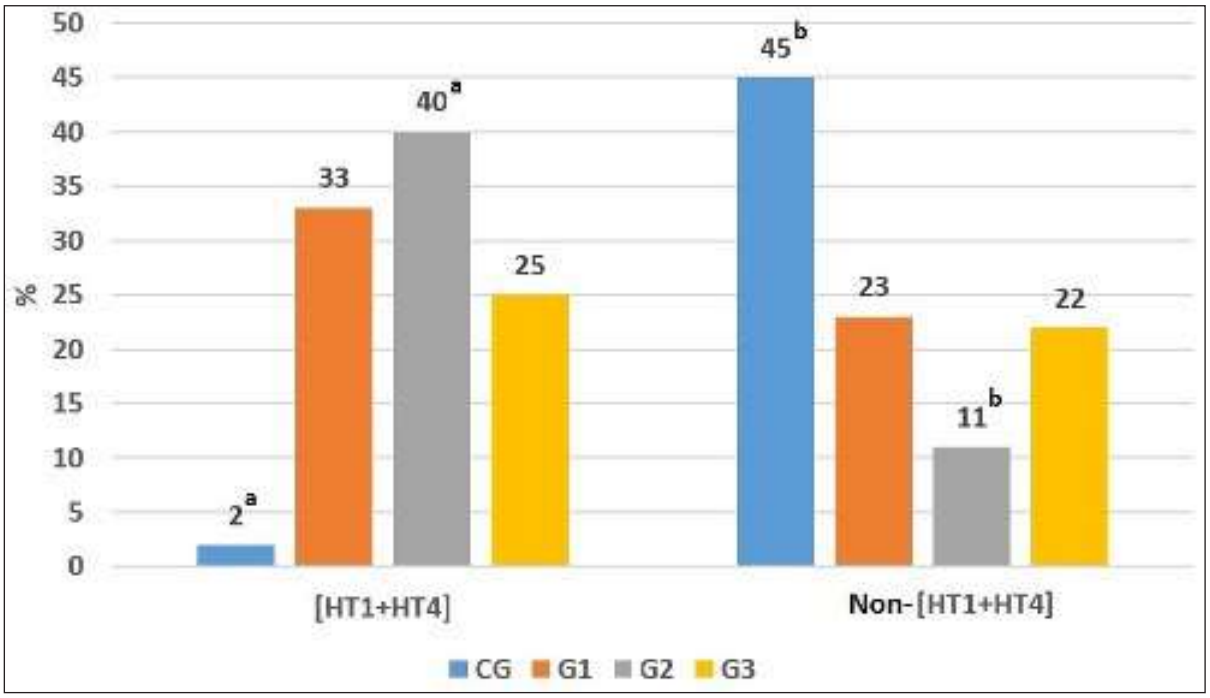

Fig. 15. The clinical status structure (%) of the pooled group [HT1+HT4] (N=45) and the non-[HT1+HT4] group (N=65). [a,b] – Each subscript letter denotes the subsets of the corresponding studied groups, whose column proportions do not differ significantly from each other at p<0,05 (z-test).

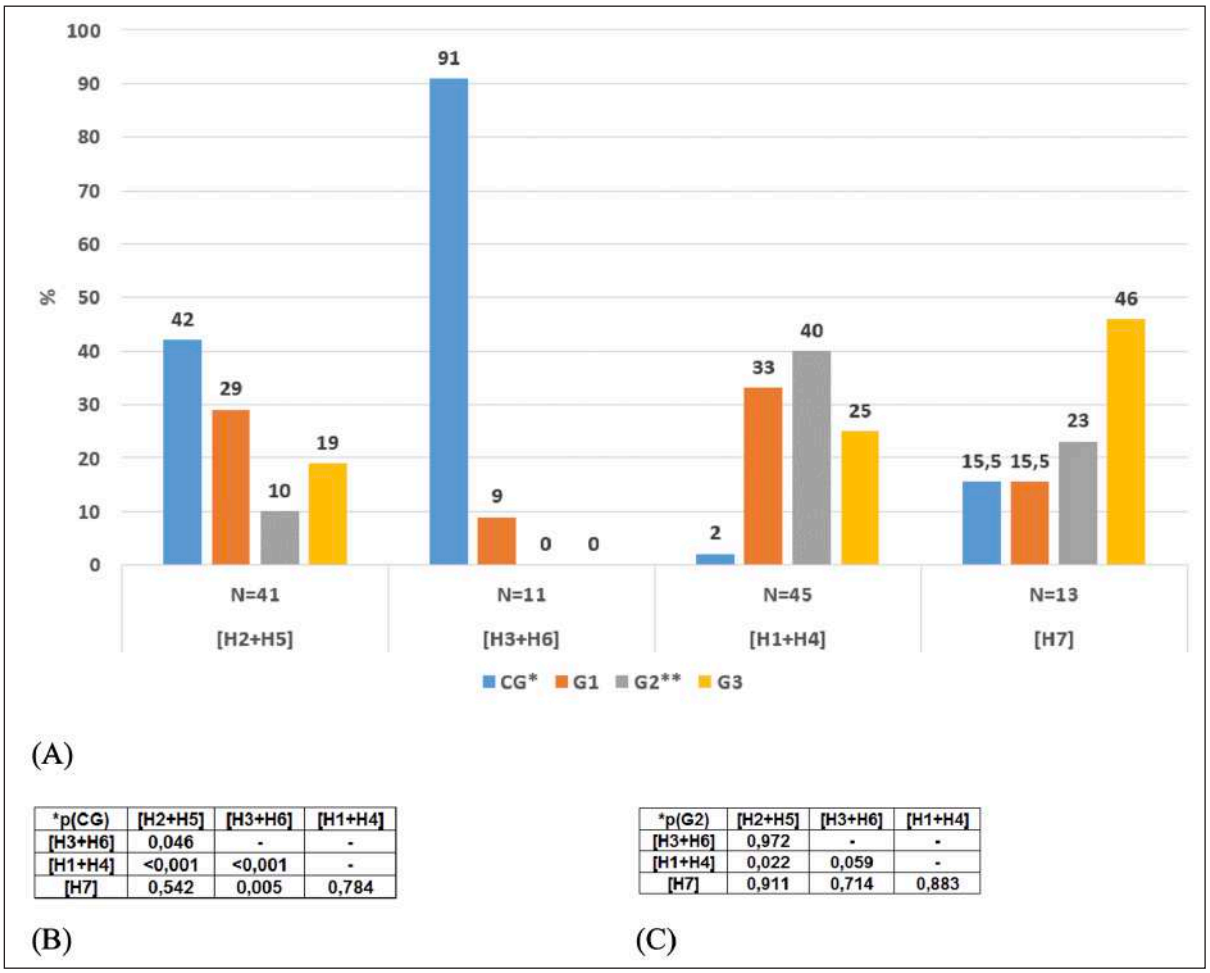

*p(CG)	[H2+H5]	[H3+H6]	[H1+H4]
[H3+H6]	0,046	-	-
[H1+H4]	<0,001	<0,001	-
[H7]	0,542	0,005	0,784

(B)

*p(G2)	[H2+H5]	[H3+H6]	[H1+H4]
[H3+H6]	0,972	-	-
[H1+H4]	0,022	0,059	-
[H7]	0,911	0,714	0,883

(C)

Fig. 16. The clinical status structure (%) of the pooled groups [HT2+HT5], [HT3+HT6], [HT1+HT4], and [H7] (A). The significance of difference between the groups by CG (B) and G2 (C) frequency.

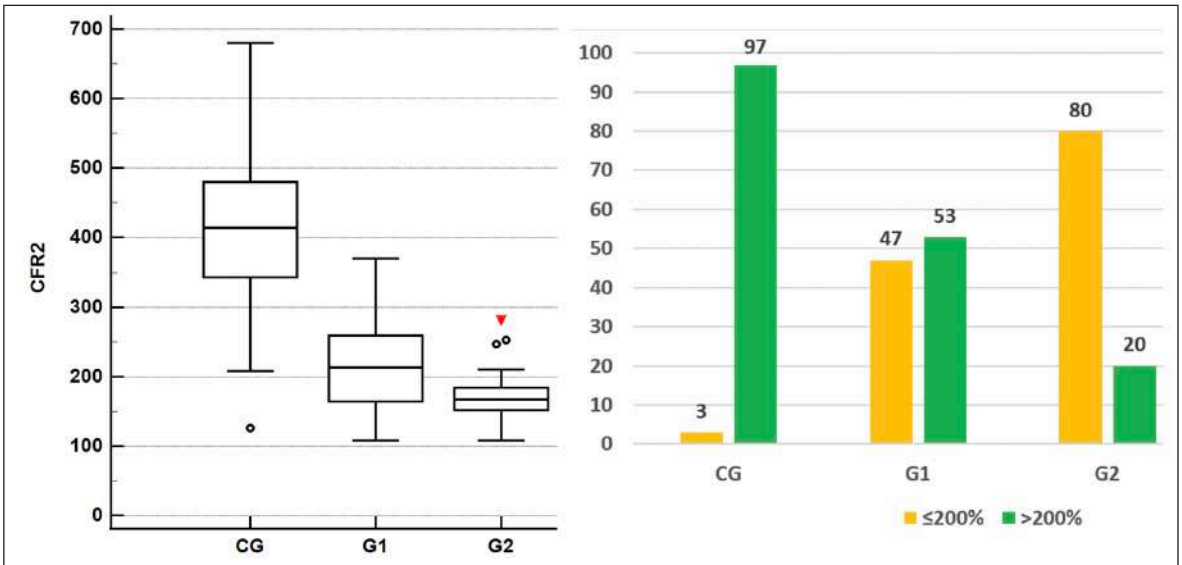

p(CFR2)	CG	G1	G2
G1	<0,001	-	-
G2	<0,001	0,126	-
G3	<0,001	1,000	0,053

(A)

p(CFR2$_{<200\,\%}$)	CG	G1	G2
G1	<0,001	-	-
G2	<0,001	0,146	-
G3	<0,001	1,000	0,347

(B)

Fig. 17. CFR2 (%) (A) and the frequency of CFR2$_{<200\,\%}$ (B) in G_1-G_3 patients and controls (box-and-whiskey plots; the significance of difference (p[CFR2] and p[CFR2$_{<200\,\%}$], respectively) between the studied groups)

Parameters	CD	CalA	CalV	LenA	LenV	VelA	VelV
LDP (M)	-0,048	0,116	0,002	-0,115	-0,100	-0,162	-0,120
LDP (SD)	**0,204**	-0,057	-0,004	**0,289**	**0,263**	**0,217**	**0,224**
LDP (CV)	**0,281**	**-0,210**	-0,004	**0,468**	**0,491**	**0,410**	**0,495**
CFR1	**0,562**	**-0,197**	0,005	**0,439**	**0,392**	**0,637**	**0,513**
CFR2	**0,513**	-0,029	0,064	**0,431**	**0,428**	**0,635**	**0,572**
AmaxE	**0,313**	**0,261**	**0,202**	0,053	0,124	**0,479**	**0,588**
AmaxN	0,065	**0,204**	0,109	**0,225**	**0,329**	**0,291**	**0,419**
AmaxM	**0,388**	**0,296**	**0,340**	**0,432**	**0,558**	**0,470**	**0,782**
AmaxR	**-0,226**	**0,227**	0,070	**-0,387**	**-0,359**	**-0,759**	**-0,470**
AmaxC	-0,181	**0,215**	0,075	**-0,434**	**-0,429**	**-0,237**	**-0,269**

Fig. 18. The correlations of LDF and NFC parameters. All the significant correlations are bold (at p<0,05).

and the laser-based techniques, particularly laser Doppler flowmetry (LDF) [12, 13]. In addition, there are data on the purposeful assessment of coronary microvascular dysfunction in COVID-19 patients and post-COVID-19 survivors [14-16], being, however, of limited availability to be obtained in routine clinical settings.

At the same time, one should be concerned over the lacking of data regarding the use of non-invasive tests for the assessment of peripheral microvascular flow and morphology, in particular NVC/LDF, in stable coronary artery disease (SCAD) patients with concomitant COVID-19. Therefore, there is an obvious need to extend our knowledge as to the clinical application of such more accessible technologies in the routine management of SCAD patients in the acute phase of SARS-CoV-2 infection, and those recovered from COVID-19.

THE AIM

The aim of the study was to evaluate the alterations in microcirculation of SCAD patients with concomitant COVID-19.

MATERIALS AND METHODS

The present cross-sectional study consecutively enrolled and analyzed the data from 55 patients with SCAD (including those with concomitant COVID-19 [n=25]), and 25 patients with SARS-CoV-2 infection without SCAD, during the period 10 Dec 2019 – 31 Dec 2022. We also enrolled 30 relatively healthy volunteers, being free from previous SARS-CoV-2 infection, and non-vaccinated against COVID-19 prior to the study (Fig. 1). The principal aspects of the study design, particularly the exclusion criteria, and the clinical and certain instrumental characteristics of the enrolled persons have been presented earlier [17].

Table I. The hemodynamic microcirculatory types in the enrolled sample (N=110) (adapted from [23, 24])

HT	LDP_M (a.u.)	Basal MF	CFR1 (%)	MVR	Description (type)	n (%)
HT1	<4,5	↓	<200	↓*	Congestion-stasis (CS)	26 (23,6)
HT2	<4,5	↓	200-300	N	Mixed	36 (32,7)
HT3	<4,5	↓	>300	↑**	Spastic	7 (6,4)
HT4	4,5-6,5	N	<200	↓*	Mixed	19 (17,3)
HT5	4,5-6,5	N	200-300	N	Normal	5 (4,6)
HT6	4,5-6,5	N	>300	↑**	Mixed	4 (3,6)
HT7	>6,5	↑	<200	↓*	Hyperemic	13 (11,8)

Note: MF – microvascular flow; MVR – microvascular reactivity; N – normal; ↓ – reduced; ↑ – increased; * – hyporeactivity; ** – hyperreactivity

NVC was performed by the use of a digital biomicroscope, with a dedicated software for image analysis, according to the standardized procedures [18, 19]. Following the application of maple oil, the right index finger (the eponychium) was examined. Other fingers (except the thumbs) bilaterally could be also examined, as required. The following static parameters were assessed: capillary density (CD) per 1 mm^2; the caliber (diameter) of the arteriolar and venular parts of the capillary loop (Cal_A and Cal_V, respectively); and the length of the arteriolar and venular parts of the capillary loop (Len_A and Len_V, respectively). In addition, the dynamic parameters were assessed, namely the blood flow (red blood cells (RBC) movement) velocity in the arteriolar and venular parts of the capillary loop (Vel_A and Vel_V, respectively).

LDF, being an optical technique for estimation of microcirculation, based on the Doppler principle [20], has been performed by the use of computerized laser Doppler flowmeter in accordance with the available principles and guidelines [20-24]. The laser probe was applied on the left extensor side forearm skin (in the midline, 4 cm above the basis of styloid processes, perpendicular to the skin surface), known to be lack of arterio-venous (AV) anastomoses, and the LDF signal was recorded for 10 minutes.

At the first step, we measured the parameters characterizing the average basal cutaneous microvascular flow (per patient or control): the mean value of (laser Doppler) perfusion (LDP) index (LDP_M; in arbitrary units [a.u.]); the standard deviation of LDP (LDP_{SD}; a.u); and the coefficient of variation of LDP (LDP_{CV}; %), calculated as a ratio (LDP_M/LDP_{SD}) x 100 %.

At the second step, we performed the wavelet analysis of the basal LDF signal and measured the (maximal) amplitude of blood flow oscillations of different frequency bands, reflecting the series of mechanisms related to the microcirculatory blood flow regulation, namely the following: the endothelial oscillations ($A_{max}E$) (0,005-0,021 Hz), representing the endothelium activity in terms of both nitric oxide (II) (NO)-dependent and -independent ways of vascular tone regulation; the neurogenic oscillations ($A_{max}N$) (0,021-0,052 Hz), reflecting the impact of neural (sympathetic) innervation on cutaneous blood flow; the myogenic oscillations ($A_{max}M$) (0,052-0,145 Hz), corresponding to (precapillary) vascular smooth muscles activity; the respiratory ($A_{max}R$) (0,145-0,6 Hz) and cardiac (pulse) ($A_{max}C$) (0,6-2 Hz) oscillations, representing, respectively, the influence of macrohemodynamics (heart rate, pulse wave) and movement of the thorax («respiratory pump») on the microvascular blood flow. The $A_{max}E$, $A_{max}N$ and $A_{max}M$ characterize the active mechanisms of microcirculatory flow modulation, whereas $A_{max}R$ and $A_{max}C$ are considered as passive ones [22-24].

After the measurement of basal microvascular flow, the occlusion functional test was performed. A pressure cuff was placed on the upper left, with the following steps of the test: the basal flow recording (for 1 minute); then the pneumatic cuff rapid inflation up to 200 mm Hg (or 50 mm Hg higher than the value of systolic blood pressure indicated by the participant) and holding for 3 minutes; and, finally, the cuff rapid deflation with continuous blood flow recording for the next 6 minutes [20, 23]. After the cuff release, one can observe a short period of the rise of perfusion, reflecting the maximum filling of microcirculatory bed with blood, referred to as «post-occlusive reactive hyperemia» (PORH). PORH, in general, characterizes the whole microcirculatory blood filling capacity, being also an accepted parameter of the endothelium function, namely the endothelium-dependent mechanisms of microvascular relaxation [23, 25]. According to the occlusion test results, we measured the capillary flow reserve (CFR1) as a ratio of the maximal flow (during the PORH period) to the basal flow (in %). The normal CFR1 was considered to be >200 % [23, 24].

The pharmacological provocative test (1 % nitroglycerin iontophoresis protocol) was performed 15 minutes after the occlusion test according to previously

described principles [23, 26], with the following steps: the basal flow recording (for 1 minute); then the flow recording during the iontophoresis for 3 minutes; and, finally, the continuous blood flow recording after the stop of iontophoresis for the next 6 minutes. The nitroglycerin iontophoresis test is purposed to assess the endothelium-independent microvascular relaxation, induced by the direct effect of exogenous NO upon the capillary smooth myocytes [23]. According to the pharmacological provocative test results, we measured the capillary flow reserve (CFR2) as a ratio of the maximal flow (on the top of nitroglycerin iontophoresis) to the basal flow (in %). The normal CFR2 was conventionally considered to be >200 %.

According to the proposed LDP_M grades (<4,5; 4,5-6,5; and ≥6,5 a.u.; LDPM <4,5 a.u. referred to as «reduced flow») [24], and considering the proposed CFR1 patterns (<200 %; 200-300 %; and >300 % [$CFR1_{<200\,\%}$, $CFR1_{200\text{-}300\,\%}$ and $CFR1_{>300\,\%}$, respectively]) [23, 24], the 7 microcirculatory hemodynamic types (HTs) were identified and summarized in Table I.

We used the certain statistical software programs for the data analysis, namely Statistica v. 14.0.0.15 (TIBCO Software Inc., USA), IBM SPSS Statistics v. 27.0 (Armonk, NY: IBM Corp., USA), MedCalc v. 22.001 (MedCalc Software Ltd., Belgium), MedStat v. 5.0 and EZR 1.61. Quantitative variables were presented as Me (IQR), and qualitative ones – as absolute and relative (%) frequency (with 95 % confidence interval (CI), as required). To compare the quantitative variables, we used Kruskal-Wallis H test with the following *post hoc* Mann-Whitney U-test (considering the Bonferroni correction). To compare the qualitative variables, we used the χ^2 test with the following z-test, as required, or with *post hoc* Marascuilo-Liakh-Gurianov procedure, and Fisher`s exact test (for «2x2» tables). The relationship between the quantitative variables was determined by the use of Spearman`s rank coefficient of correlation (ρ). A 2-tailed p<0,05 was considered statistically significant (considering the Bonferroni correction) (Table I).

RESULTS

The description of participants` profiles and comparison of clinical characteristics between the studied groups have been presented earlier [17].

The results of NFC were indicative for the capillary rarefaction in G_1-G_3, as compared to controls (Fig. 2).

The Cal_A tended to be lower in G_1 (vs. CG), and was the highest in G_3 (vs. CG, G_1 and G_2). Besides, G_1-G_2-G_3 demonstrated a trend towards the increase in Cal_A (Fig. 3A). In addition, the Cal_V was lower in G_1 (vs. CG), being, however, comparable between CG, G_2 and G_3 (Fig. 3B).

All three groups of patients demonstrated the decrease of Len_A and Len_V (vs. CG) (Fig. 4), with the lowest Len_A value observed in G_3 (Fig. 4A).

Moreover, G_1-G_3 demonstrated the drop of Vel_A and Vel_V, in contrast to controls (Fig. 5), with the lowest Vel_A value observed in G_2 (Fig. 5A) and Vel_V – in G_1 patients (Fig. 5B). Finally, G_1-G_2-G_3 demonstrated a trend towards the increase in Vel_V (Fig. 5B).

The studied groups were comparable in terms of LDP_M, as well as regarding the frequency of LDP_M patterns (Fig. 6). However, G_3, in contrast to CG and G_1-G_2, was characterized by numerically, bot non-significantly lower frequency of LDP_M <4,5 a.u. pattern, and higher of LDP_M >6,5 a.u. category, being more «harmonized» by the presence of all three LDP_M patterns (Fig. 6). Moreover, the LDP variability was reduced in all the groups of patients, as compared to controls (in G_1-G_3 – by LDP_{CV}, and G_2 – by LDP_{SD} also) (Fig. 7).

The $A_{max}E$ was reduced in G_1 and G_2, in comparison with controls, with the lowest value observed in G_2. At the same time, we did not observe a decrease of $A_{max}E$ in G_3, which was even slightly higher than that in CG (Fig. 8). In addition, G_1 and G_2 demonstrated a drop in $A_{max}N$ (vs. CG and G_3), which was comparable between controls and «isolated» COVID-19 patients (G_3) (Fig. 9). Patients from G_1-G_3 presented with a decrease of $A_{max}M$ (vs. CG), with the lowest value registered in G_1 (Fig. 10). We detected a rise of $A_{max}R$ in G_1-G_3 (vs. CG), which tended to be the most pronounced in G_2 (Fig. 11). Finally, despite the increase of $A_{max}C$ in G_1 and G_3 (vs. CG), G_2 did not present such a tendency (Fig. 12).

The results of the occlusion test were evident for the decrease of CFR1 in all three groups of patients, as compared to CG (Fig. 13A). The $CFR1_{200\text{-}300\,\%}$ pattern was the most prevalent among controls, being more frequent in comparison to G_2, where it constituted the minority of cases (57 % vs. 16 %, respectively; p=0,035) (Fig. 13B). On the contrary, the frequency $CFR1_{<200\%}$ pattern was higher in all three groups of patients, as opposed to CG, where it constituted the minority of cases (10 % vs. 57 % in G_1 (p=0,003); 84 % in G_2 (p<0,001); and 68 % in G_3 [p<0,001]). In addition, the $CFR1_{<200\%}$ pattern was the most prevalent (numerically, but non-significantly) in G_2, in comparison to G_1 and G_3 (Fig. 13B). At last, the $CFR1_{>300\,\%}$ pattern constituted one-third of the controls (33 % [95 **%** CI 17-52 %]), being significantly higher vs. G_1 (3 % [95 % CI 0-13 %]; p=0,040), G_2 (0 [95 % CI 0-7 %]; p=0,010) and G_3 (0 [95 % CI 0-7 %]; p=0,010) (Fig. 13B).

According to the HTs distribution in the studied groups (Fig. 14), CG was characterized by the prevalence of HT2 (mixed type with LDP_M <4,5 a.u. and preserved endothelium-dependent microcirculatory reactivity) and HT3 (spastic type) (67 % in total). In turn, the half

of patients with «isolated» SCAD presented with a pattern of LDP_M ≤6,5 a.u. and impaired microvascular reactivity (including CS-type (HT1) and mixed HT4), and one-third – with HT2. Moreover, HT1 and HT4 altogether prevailed in G_2 and constituted 72 % of the cases. At last, patients with «isolated» COVID-19 (G_3) presented with 3 major HTs, namely H2, H4 and HT7 (the hyperemic one) (Fig. 14).

The studied groups differed significantly in terms of the frequency of HT1 and HT4 cases. In particular, HT1 was more prevalent in G_1 (33 %) and G_2 (52 %), as compared to CG (3 %; p=0,040 and p<0,001, respectively). And the frequency of HT4 was higher in G_3 (36 % [95 % CI 18-56 %]), in contrast to CG (0 [95 % CI 0-6 %]; p=0,004) (Fig. 14).

Importantly, the group of patients with the pooled pattern [HT1+HT4], being characterized, as previously mentioned, by LDP ≤6,5 a.u. and impaired microvascular reactivity ($CFR1_{<200\%}$), demonstrated the higher frequency of SCAD and COVID-19 constellation (40 %), as against 11 % in the pooled non-[HT1+HT4] group (p<0,001), including, predominantly, the cases of LDP ≤6,5 a.u. with preserved microvascular reactivity ($CFR1_{200\text{-}300\,\%}$ and $CFR1_{>300\,\%}$) (52 of 65 [80 %]). Of note, the controls constituted only 2 % in the pooled group [HT1+HT4] (vs. 45 % in non-[HT1+HT4] group [p<0,001]) (Fig. 15).

Furthermore, while pooling H2 and H5 (based on the presence of normal microvascular reactivity [$CFR1_{200\text{-}300\,\%}$]), and combining H3 and H6 (based on LDP ≤6,5 a.u. and microvascular «hyperreactivity» [$CFR1_{>300\,\%}$]), as well as considering HT7 as a separate (hyperemic) type, the frequency of G_2 was higher in the pooled [H1+H4] group vs. the pooled [H2+H5] pattern, and tended to be higher vs. H7 (Fig. 16). In addition, the pooled group [H3+H6] was represented almost entirely by the controls (10 of 11 cases).

The results of the pharmacologic provocation test (nitroglycerin iontophoresis) demonstrated the decrease of CFR2 in G_1-G_3, as opposed to CG (Fig. 17A). Furthermore, G_2 was characterized by the predominance of $CFR2_{<200\,\%}$ cases, which were more frequent as opposed to CG (significantly), G_1 and G_3 (numerically, but non-significantly) (Fig. 17B).

The NFC data, characterizing the capillary remodeling and blood velocity (in arterial and venous parts of the capillary loop), in general, correlated with microvascular flow parameters, obtained by means of LDF (Fig. 18). In particular, the moderate (or close to moderate) positive correlations were observed between CD and CFR1/CFR2; Len_A and LDP_{CV}; Len_V and $LDP_{CV}/A_{max}M$; Vel_A and $CFR1/CFR2/A_{max}E/A_{max}M$; Vel_V and $LDP_{CV}/CFR1/CFR2/A_{max}E$; and negative – between Vel_V and $A_{max}R$ (Fig. 18). In addition, we identified a strong positive correlation of Vel_V with $A_{max}M$; and negative – between Vel_A and $A_{max}R$ (Fig. 18).

DISCUSSION

Currently available data have given us a new set of insights on the impact of SARS-CoV-2 on the structural and functional aspects of microcirculation [10-13], raising further questions regarding the alterations in the active and passive mechanisms of microvascular blood flow regulation, and their comprehensive evaluation in the management of COVID-19 patients, including those with SCAD. These issues could be, at least partly, bypassed by the use of laser-based technologies, particularly LDF, for non-invasive assessment of microcirculatory perfusion, bringing the valuable data in addition to NVC [20-24].

The presently obtained NVC results were evident for the changes in capillary bed, namely its remodeling (the capillary rarefication, along with dilation, narrowing or shortening of the capillary loops` parts) and functional alterations (the drop in blood flow in both loop compartments), occurred universally across the entire spectrum of the enrolled patients [2, 11, 12, 18, 19, 27, 28]. In particular, patients with «isolated» COVID-19 presented with the most advanced dilation and shortening of the arteriolar part of the capillary loop, along with the least slowing of the venular flow, corresponding with currently available data regarding the impact of SARS-CoV-2 infection upon the capillaries [2, 11, 12, 27, 28]. In contrast, «isolated» SCAD patients demonstrated the narrowest arteriolar part and the lowest Vel_V among the enrolled subjects. At last, the slowest RBC motion in the arteriolar part of the capillary loop was inherent to SCAD patients with concomitant COVID-19.

Despite the fact that presently studied groups of controls and patients were comparable by the average perfusion index value, we observed the decrease in LDP variability in G_1-G_3, suggesting the deterioration of the dynamic component of microvascular flow regulation in both SCAD and COVID-19, as well as their constellation [22-24].

The wavelet analysis revealed a decrease of $A_{max}E$ in both G_1 and G_2, indicating not only the microvascular endothelium to be functionally compromised in both non-infected and infected SCAD patients, but also assuming the SARS-CoV-2 infection to be superimposed on the preexisting endothelial dysfunction, that would probably provide a basis for its further aggravation in SCAD patients with concomitant COVID-19. At the same time, patients with «isolated» COVID-19 did not demonstrate a depressed $A_{max}E$ value, as compared

to controls and SCAD groups, suggesting the more advanced «plasticity» of endothelial barrier function regulation and its higher compensatory ability to adapt itself to the homeostasis disruption in the case of lesser comorbidity burdened COVID-19 patients [3, 8, 9].

A drop in $A_{max}N$ and $A_{max}M$, being detected in both G_1 and G_2, and considering the registration skin site lacking of AV-anastomoses, reflects the rise of sympathetic activity, and microvascular resistance (the increase in precapillary smooth muscles tone), with the consequent decrease in the nutritive blood flow. In turn, the increase of $A_{max}R$ in G_1-G_3 could be the sign of venular outflow impairment and, therefore, microcirculatory congestion, tended to be the most pronounced in SCAD patients with concomitant SARS-CoV-2 infection. Moreover, the sympathetic overactivity, along with presumably decreased arterial wall compliance, could underlie the rise in $A_{max}C$ in SCAD patients [22-24]. However, patients with SCAD and concomitant COVID-19 did not present the increase in $A_{max}C$, as compared to controls, that could be, at least partly, related to the most pronounced left ventricular (LV) contractility decline in G_2, in contrast to G_1 and G_3 (see [17]). Finally, as of G_3, numerically (but non-significantly) more prevalent LDP >6,5 a.u. pattern, along with comparable $A_{max}N$, the least decreased $A_{max}M$ and the increased $A_{max}C$ (all three parameters vs. CG), indicate the increased perfusion due to the lower (as compared to SCAD) precapillary resistance [22-24], being presently observed in «isolated» SARS-CoV-2 infection, and probably linked to the COVID-19-related hyperproduction of proinflammatory cytokines [29].

Facing the evidence on the multifaceted nature of microcirculatory alterations [20-24], and accounting for the presently obtained data, the patients with SCAD, COVID-19 and their constellation are supposed to demonstrate the various patterns of microvascular flow disturbances, being characterized by the presence of «spastic», «congestive» and «hyperemic» properties. However, a more comprehensive approach to the evaluation of microvascular flow disturbances requires the series of functional tests to be additionally performed [20, 23, 24].

The presently obtained results of the vascular occlusion test and pharmacologic provocation test (nitroglycerin iontophoresis) demonstrated the decrease of CFR1 and CFR2 in G_1-G_3 (vs. CG), suggesting both endothelium-dependent and -independent mechanisms of microcirculatory reactivity to be universally affected in all the studied conditions [3, 8, 9, 23, 24, 30].

The combined analysis of both LDP and CFR1 patterns revealed the predomination of HT2 (mixed type reduced perfusion and preserved microcirculatory reactivity) and HT3 (spastic type) among controls, reflecting, at least partly, the known fact regarding the vasculature to be normally in a relatively constricted state [21].

At the same time, the «isolated» COVID-19 group was characterized by the presence of HTs with the wide spectrum of properties, being likely related to the multifaceted pathophysiology of SARS-CoV-2 infection [1, 4, 29, 30]. In particular, interleukin (IL)-6 is known to promote a vascular remodeling via the increased transforming growth factor-β_1-mediated matrix metalloproteinases (MMPs) (2 and 3 types) signaling. In turn, the activation of MMPs contributes to the disruption in endothelial vasodilatory function, which is tightly linked to the stability of endothelial glycocalyx. The pro-inflammatory and pro-oxidative conditions, being clearly evident in COVID-19, are associated with the endothelial glycocalyx structural alterations, and its damage by pro-inflammatory cytokines (such as IL-1 and IL-6) leads to the increased vascular permeability with the consequent interstitial fluid shift and generalized edema [31, 32].

Finally, the SCAD patients with concomitant COVID-19 presented with the predomination of pooled «congestion-like» [HT1+HT4] pattern, being more frequent than in «isolated» SCAD group. In addition, the combined SCAD/COVID-19 cases occurred more often in the pooled [HT1+HT4] group, as compared to other HTs, namely the group with pooled [HT2+HT5] pattern. These data prompt us to make an assumption that the shift towards congestive or «congestive-like» microvascular alterations in SCAD patients with concomitant SARS-CoV-2 infection is supposed to be the result of a dramatic additive effect of COVID-19-related pathomechanisms of vascular remodeling *per se*, along with the superimposition of coronavirus infection on the preexisting SCAD-associated endothelial dysfunction, and the probable myocardial damage leading to a more advanced decrease in LV contractility, being also demonstrated in our previous work [17].

Generally, the deterioration of the capillary bed structural and functional properties, detected by NVC, correlated with the alterations in the active mechanisms of microvascular flow regulation, and were associated with the changes in the passive ones. At the same time, the combined analysis of both NVC and LDF data allows us to provide an averaged integral evaluation of the «portraits» of patients with different studied conditions.

In particular, the abovementioned changes in the capillary bed and the LDF signal properties are focused on the shift towards «hyperemic» microcirculatory alterations, being specifically attributed to the «isolated» COVID-19 averaged phenotype.

At the same time, the «isolated» SCAD group represented a phenotype of the «increased arterial re-

sistance», being reflected, *inter alia*, by the narrowing of the arteriolar part of capillary loops. Importantly, such a phenotype included the cases of both reduced and preserved microvascular reactivity. Here, it worth be considered the strong correlation of the reduced myogenic flow oscillations, being the most advanced in «isolated» SCAD patients, and the drop of venular blood flow, suggesting indirectly the reduce of arteriolar capillary flow related to the increased precapillary resistance. We surmise also that the reversibility of the observed microcirculatory alterations in SCAD patients seems to depend on the baseline structural and functional properties of the arterial vascular bed, namely the state of endothelium, known to be affected in the setting of atherosclerosis, hypertension, diabetes mellitus etc. [33].

Finally, the potential aggravation of the preexisted endothelial dysfunction in SCAD patients under the impact of SARS-CoV-2 infection seems to contribute to a more frequent and more pronounced microcirculatory congestion, as compared to that in patients with both «isolated» conditions, being evident also by the slowest RBC movement in the arteriolar part of the capillary loops. It should be emphasized the strong correlation of Vel_A with the amplitude of respiratory oscillations, tended to be the highest in SCAD patients with concomitant SARS-CoV-2 infection, which was an additional argument for a shift towards the more advanced congestive microcirculatory alterations in the settings of such an associated pathology. Furthermore, the LV systolic function impairment, observed previously in G_2 [17], due to probable COVID-19-related myocardial damage, could enhance the severity of microcirculatory congestion in an additive manner.

The present study is subjected to several limitations, including its cross-sectional design, modest sample size, and the enrollment of unvaccinated patients and controls. Moreover, the limitations of NVC and LDF should be also considered. In particular, NVC is not the examination of choice for the evaluation of the blood flow, thus requiring to be complemented with other dedicated methods for better peripheral perfusion measurements [10]. Furthermore, the limitations of LDF technique are related to the standardization issues and the necessity of the control group enrollment [20-24].

Because of the partial overlapping between the studied groups in terms of different HTs, further research is highly necessary to provide an advanced phenotyping of such a specific pattern of SCAD patients with concomitant COVID-19. This issue could be, at least partly, resolved by the study of microcirculatory data relationships with the broad spectrum of patients` characteristics, including the parameters of central hemodynamics, and considering the applied pharmacotherapy, at baseline and follow-up. Such an approach to the data analysis is justified considering the purpose to improve the management of SCAD patients, suffering from SARS-CoV-2 infection, particularly regarding the better risk stratification for COVID-19-related complications (including the thromboembolic events) and post-COVID sequelae, with the following personalization of treatment and preventive strategies.

CONCLUSIONS

SCAD patients with concomitant COVID-19 demonstrated a wide spectrum of microcirculatory disturbances, particularly the remodeling of the capillary bed, the alterations in the active (endothelium-dependent and -independent) mechanisms of microvascular flow regulation, and the drop in arteriolar and venular RBC movement velocity. At the same time, the profile of SCAD and COVID-19 constellation, as opposed to the «isolated» course of both conditions, was characterized by the predomination of patients, possessing a hemodynamic microcirculatory CS-type or a mixed pattern of reduced microvascular reactivity. Furthermore, the pooled microcirculatory hyporeactive profile was presented with the cases of combined SCAD and SARS-CoV-2 infection to a greater extent, than in the pooled profile with predominantly preserved microvascular reactivity. There is a need for the methods of non-invasive evaluation of microcirculatory system properties and the assessment of microvascular reactivity to be broadly applied while management of SCAD patients, suffering from COVID-19.

REFERENCES

1. Rabaan AA, Smajlović S, Tombuloglu H et al. SARS-CoV-2 infection and multi-organ system damage: A review. Biomol Biomed. 2023;23(1):37-52. doi: 10.17305/bjbms.2022.7762.
2. Mondini L, Confalonieri P, Pozzan R et al. Microvascular Alteration in COVID-19 Documented by Nailfold Capillaroscopy. Diagnostics (Basel). 2023;13(11):1905. doi: 10.3390/diagnostics13111905.
3. Xu SW, Ilyas I, Weng JP. Endothelial dysfunction in COVID-19: an overview of evidence, biomarkers, mechanisms and potential therapies. Acta Pharmacol Sin. 2023;44(4):695-709. doi: 10.1038/s41401-022-00998-0.
4. Nicolai L, Kaiser R, Stark K. Thromboinflammation in long COVID-the elusive key to postinfection sequelae? J Thromb Haemost. 2023;21(8):2020-2031. doi: 10.1016/j.jtha.2023.04.039.

5. Yousefimoghaddam F, Goudarzi E, Ramandi A, Khaheshi I. Coronary artery calcium score as a prognostic factor of adverse outcomes in patients with COVID-19: a comprehensive review. Curr Probl Cardiol. 2023;48(8):101175. doi: 10.1016/j.cpcardiol.2022.101175.
6. Szarpak L, Mierzejewska M, Jurek J et al. Effect of Coronary Artery Disease on COVID-19-Prognosis and Risk Assessment: A Systematic Review and Meta-Analysis. Biology (Basel). 2022;11(2):221. doi: 10.3390/biology11020221.
7. Boulos PK, Freeman SV, Henry TD et al. Interaction of COVID-19 With Common Cardiovascular Disorders. Circ Res. 2023;132(10):1259-1271. doi: 10.1161/CIRCRESAHA.122.321952.
8. Kovanen PT, Vuorio A. SARS-CoV-2 reinfection: Adding insult to dysfunctional endothelium in patients with atherosclerotic cardiovascular disease. Atheroscler Plus. 2023;53:1-5. doi: 10.1016/j.athplu.2023.06.002.
9. Passi R, Brittan M, Baker AH. The role of the endothelium in severe acute respiratory syndrome coronavirus 2 infection and pathogenesis. Curr Opin Physiol. 2023;34:100670. doi: 10.1016/j.cophys.2023.100670.
10. Natalello G, De Luca G, Gigante L et al. Nailfold capillaroscopy findings in patients with coronavirus disease 2019: Broadening the spectrum of COVID-19 microvascular involvement. Microvasc Res. 2021;133:104071. doi: 10.1016/j.mvr.2020.104071.
11. Karahan S, Aydin K, Cetinkaya A, Sirakaya HA. Nailfold Videocapillaroscopy in Patients with COVID-19-associated Pneumonia in Intensive Care Units. J Coll Physicians Surg Pak. 2022;32(4):455-460. doi: 10.29271/jcpsp.2022.04.455.
12. Sabioni L, De Lorenzo A, Castro-Faria-Neto HC et al. Long-term assessment of systemic microcirculatory function and plasma cytokines after coronavirus disease 2019 (COVID-19). Braz J Infect Dis. 2023;27(1):102719. doi: 10.1016/j.bjid.2022.102719.
13. Sabioni L, De Lorenzo A, Lamas C et al. Systemic microvascular endothelial dysfunction and disease severity in COVID-19 patients: Evaluation by laser Doppler perfusion monitoring and cytokine/chemokine analysis. Microvasc Res. 2021;134:104119. doi: 10.1016/j.mvr.2020.104119.
14. Malahfji M, Crudo V, Ahmed AI et al. Coronary microvascular dysfunction and COVID-19: implications for long COVID patients. J Nucl Cardiol. 2022;1-3. doi: 10.1007/s12350-022-03073-7.
15. Çalışkan M, Baycan ÖF, Çelik FB et al. Coronary microvascular dysfunction is common in patients hospitalized with COVID-19 infection. Microcirculation. 2022;29(4-5):e12757. doi: 10.1111/micc.12757.
16. Rola P, Włodarczak A, Włodarczak S et al. Invasive assessment of coronary microvascular dysfunction in patients with long COVID: Outcomes of a pilot study. Kardiol Pol. 2022;80(12):1252-1255. doi: 10.33963/KP.a2022.0239.
17. Netiazhenko VZ, Mostovyi SI, Safonova OM et al. Intracardiac hemodynamics, cerebral blood flow and microembolic signal burden in stable coronary artery disease patients with concomitant COVID-19. Wiad Lek. 2023;76(5 pt 2):1205-1215. doi: 10.36740/WLek202305211.
18. Lushchyk UB, Novytskyi VV, Kolosova YuO. Suchasni mozhlyvosti kapiliaroskopii [Current capabilities of capillaroscopy]. Kyiv: MPP «Istyna». 2004. https://www.researchgate.net/publication/318883496_Sucasni_mozlivosti_kapilaroskopii [date access 05.06.2023] (In Ukrainian).
19. Smith V, Herrick AL, Ingegnoli F et al. Standardisation of nailfold capillaroscopy for the assessment of patients with Raynaud's phenomenon and systemic sclerosis. Autoimmun Rev. 2020;19(3):102458. doi: 10.1016/j.autrev.2020.102458.
20. Bircher A, de Boer EM, Agner T et al. Guidelines for measurement of cutaneous blood flow by laser Doppler flowmetry. A report from the Standardization Group of the European Society of Contact Dermatitis. Contact Dermatitis. 1994;30(2):65-72. doi: 10.1111/j.1600-0536.1994.tb00565.x.
21. Fullerton A, Stücker M, Wilhelm KP et al. Guidelines for visualization of cutaneous blood flow by laser Doppler perfusion imaging. A report from the Standardization Group of the European Society of Contact Dermatitis based upon the HIRELADO European community project. Contact Dermatitis. 2002;46(3):129-140. doi: 10.1034/j.1600-0536.2002.460301.x.
22. Saha M, Dremin V, Rafailov I et al. Wearable Laser Doppler Flowmetry Sensor: A Feasibility Study with Smoker and Non-Smoker Volunteers. Biosensors (Basel). 2020;10(12):201. doi: 10.3390/bios10120201.
23. Goltsov A, Anisimova AV, Zakharkina M. Bifurcation in Blood Oscillatory Rhythms for Patients with Ischemic Stroke: A Small Scale Clinical Trial using Laser Doppler Flowmetry and Computational Modeling of Vasomotion. Front Physiol. 2017; 8: 160. doi: 10.3389/fphys.2017.00160.
24. Makolkin V.I., Podzolkov V.I., Bran'ko V.V. Mikrotsirkulyatsiya v kardiologii. [Microcirculation in cardiology]. Moscow: Vizart. 2004 pp.105-110.
25. Horn AG, Schulze KM, Weber RE et al. Post-occlusive reactive hyperemia and skeletal muscle capillary hemodynamics. Microvasc Res. 2022;140:104283. doi: 10.1016/j.mvr.2021.104283.
26. Iredahl F, Sadda V, Ward LJ et al. Modeling Perfusion Dynamics in the Skin During Iontophoresis of Vasoactive Drugs Using Single-Pulse and Multiple-Pulse Protocols. Microcirculation. 2015;22(6):446-53. doi: 10.1111/micc.12211.
27. Osiaevi I, Schulze A, Evers G et al. Persistent capillary rarefication in long COVID syndrome. Angiogenesis. 2023;26(1):53-61. doi: 10.1007/s10456-022-09850-9.
28. Gualtierotti R, Fox SE, Da Silva Lameira F et al. Nailfold Videocapillaroscopic Alterations as Markers of Microangiopathy in COVID-19 Patients. J Clin Med. 2023;12(11):3727. doi: 10.3390/jcm12113727.

29. Dharra R, Kumar Sharma A, Datta S. Emerging aspects of cytokine storm in COVID-19: The role of proinflammatory cytokines and therapeutic prospects. Cytokine. 2023;169:156287. doi: 10.1016/j.cyto.2023.156287.
30. Santoro L, Zaccone V, Falsetti L et al. Role of Endothelium in Cardiovascular Sequelae of Long COVID. Biomedicines. 2023;11(8):2239. doi: 10.3390/biomedicines11082239.
31. Doroszko A, Rola P, Włodarczak S et al. Coronary microvascular dysfunction in the context of long COVID-19: What is the effect of anti-inflammatory treatment? Author's reply. Kardiol Pol. 2023;81(3):320-321. doi: 10.33963/KP.a2023.0040.
32. Okada H, Yoshida S, Hara A et al. Vascular endothelial injury exacerbates coronavirus disease 2019: The role of endothelial glycocalyx protection. Microcirculation. 2021;28(3):e12654. doi: 10.1111/micc.12654.
33. Zhang Z, Li X, He J et al. Molecular mechanisms of endothelial dysfunction in coronary microcirculation dysfunction. J Thromb Thrombolysis. 2023;56(3):388-397. doi: 10.1007/s11239-023-02862-2.

The study was conducted in accordance with the basic principles of the Council of Europe Convention on Human Rights and Biomedicine, World Medical Association Declaration of Helsinki on the ethical principles for medical research involving human subjects, and current national regulations. The study protocol was approved by the local ethics committee. All the patients provided written informed consent to participate in the study.

The study was conducted as a fragment of the complex scientific projects of the Department of Propaedeutics of Internal Medicine № 1 (Bogomolets National Medical University) «Features of changes in the system of hemocoagulation in the comorbid state of coronary heart disease and hypertension, laboratory and genetic predictors of thrombotic complications» (state registration number 0118U001391; term: 2018-2020) and «Correction of changes in platelet and plasma hemostasis in patients with coronary syndromes and hypertension, taking into account the presence of comorbid pathology» (state registration number 0121U110275; term: 2021-2023), in collaboration with State Institution of Science «Research and Practical Center of Preventive and Clinical Medicine» State Administrative Department (the complex scientific project of the Scientific Department of Internal Medicine «Improvement of patient-oriented approaches to the management of patients with cardiovascular and cerebrovascular diseases with comorbid conditions, in particular in those suffered from COVID-19» [state registration number 0122U000234; term: 2022-2024]).

ORCID and contributionship:
Vasyl Z. Netiazhenko: 0000-0001-9697-4421 [A, E, F]
Serhii I. Mostovyi: 0000-0002-8783-3819 [A-D]
Olga M. Safonova: 0009-0007-8839-4268 [B]
Kyrylo O. Mikhaliev: 0000-0003-3759-6699 [C, E]

Conflict of interest:
The Authors declare no conflict of interest.

CORRESPONDING AUTHOR

Serhii I. Mostovyi
Bogomolets National Medical University
13 Taras Shevchenko Blvd, 01601 Kyiv, Ukraine
tel: +380503835120
e-mail: semostowoy@ukr.net

Received: 14.05.2023
Accepted: 22.09.2023

A - Work concept and design, **B** – Data collection and analysis, **C** – Responsibility for statistical analysis, **D** – Writing the article, **E** – Critical review, **F** – Final approval of the article